

POTENTIAL OF BRAGG GRATING SENSORS FOR AIRCRAFT HEALTH MONITORING

Nezih Mrad

Air Vehicle Research Section (AVRS), Defence R&D Canada (DRDC)
Department of National Defence (DND), National Defence Headquarters
Ottawa, ON K1A 0K2, Canada

Tel: (613) 993-6443; Fax: (613) 993-4095, Email: Nezih.mrad@drdc-rddc.gc.ca

Received July 2006, Accepted March 2007
No. 06-CSME-33, E.I.C. Accession 2952

ABSTRACT

The increased requirement to operate military platforms and aerospace structures beyond their designed life imposes heavy maintenance and inspection burden on aircraft operators and owners. In-service structural health monitoring is potentially a cost-effective approach by which service usage information can be obtained and knowledgeable decisions can be made. Advanced sensor technology, such as optical fibres, are expected to provide existing and future aircraft with added intelligence and functionality, reduced weight and cost, enhanced robustness and performance. This paper furthers the understanding of technical and practical issues related to full implementation of a fibre optic sensor based structural health monitoring system for aerospace and military platforms. It also reports experimental findings on the use of fibre Bragg grating sensors for measurement of parameters relevant to aircraft structural monitoring and smart structures; with an emphasis on the suitability of multifunctional fibre optic sensor system. Experimental evaluations revealed that Bragg grating sensors correlate well with conventional sensors technology for temperature, stain, crack growth and cure monitoring and were insensitive to pressures up to 300 psi. These sensors were determined to have minimum impact on the structural integrity when embedded parallel to host fibres into composite laminates. Recommendations on the implementation and integration of these sensors into a structural health monitoring system are also provided.

LE POTENTIEL DES CAPTEURS À FIBRES OPTIQUES À RÉSEAUX DE BRAGG POUR LA SURVEILLANCE DE L'INTEGRITÉ DE STRUCTURES AÉRONAUTIQUES

RÉSUMÉ

La demande accrue pour l'opération des plateformes militaires et des structures aérospatiales au delà de leurs durée de vie théorique impose un lourd fardeau d'entretien et d'inspection aux opérateurs et propriétaires d'avion. La surveillance de l'intégrité des structures en service est potentiellement une méthode rentable par laquelle l'information sur l'usage de service peut être obtenue et des décisions intelligentes peuvent être prises. On s'attend à ce que la technologie des capteurs avancés, telle que les fibres optiques, fournisse aux présents et futures avions une intelligence et des fonctionnalités supplémentaires, une réduction du poids et du coût, et une augmentation de la robustesse et de la performance. Cet article fournit plus de détails pour comprendre les enjeux techniques et pratiques reliées à la pleine implémentation d'un système de surveillance de l'intégrité des structures pour les plateformes aérospatiales et militaire basée sur les capteurs à fibres optiques. Il rapporte également des résultats expérimentaux sur l'utilisation des capteurs à fibres optiques à réseaux de Bragg pour mesurer des paramètres reliés à la surveillance de structures aéronautiques et des structures intelligentes avec une emphase sur la pertinence d'un système de capteurs à fibres optiques multifonctionnelles. Les évaluations expérimentales indiquent que les capteurs à fibres optiques à réseaux de Bragg corrélerent bien avec les technologies traditionnelles utilisées dans la mesure de températures, de contraintes, de propagation de fissures, et de surveillance lors de la polymérisation des matériaux composites. Ces capteurs, qui sont insensible aux pressions allant jusqu'à 300 livres par pouce carré, ont été jugé d'avoir peu d'impact sur l'intégrité structurelle lorsqu'ils sont imbriqués parallèlement aux fibres de matériaux composites. Des recommandations concernant l'exécution et l'intégration de ces capteurs dans un système de surveillance de l'intégrité structurelle sont aussi fournies.

1. INTRODUCTION

Due to economic pressure and budgeting constraints, including the very high cost of aircraft replacement, operators are faced with operating their fleets beyond their initial design life cycle. The CF-188 fleet that was introduced into service in 1984 will remain in service until the year 2018 and possibly beyond, which is 14 years beyond the aircraft original design life. In Australia, the F-111C fleet will be in service for about 20 years more than the original design life of the aircraft. With high operational demands from aging fleets, problems associated with aging wires, corrosion and high cycle fatigue have become increasingly severe. This has increased the inspection frequency, hence reducing aircraft availability. Reduction of inspection and maintenance cost could potentially be achieved through the development and integration of an advanced Structural Health Monitoring System (SHMS) that could detect, assess, and monitor the structural integrity of the aircraft, and report on incipient damage before a catastrophic failure occurs. The SHMS must be cost-effective, autonomous, distributed, reliable, robust, compact, and lightweight to gain the widespread acceptance in the aerospace industry. A schematic of a potential concept for SHMS is shown in Figure 1 [1]. This concept must have the flexibility to be retrofitted into existing aircraft structures or integrated into newly developing airframes and systems. It must also be designed for ease of integration into an overall aircraft prognostic health management (PHM) system. One of the primary challenges in implementing such a system is the selection and placement of suitable local and global detection and monitoring techniques.

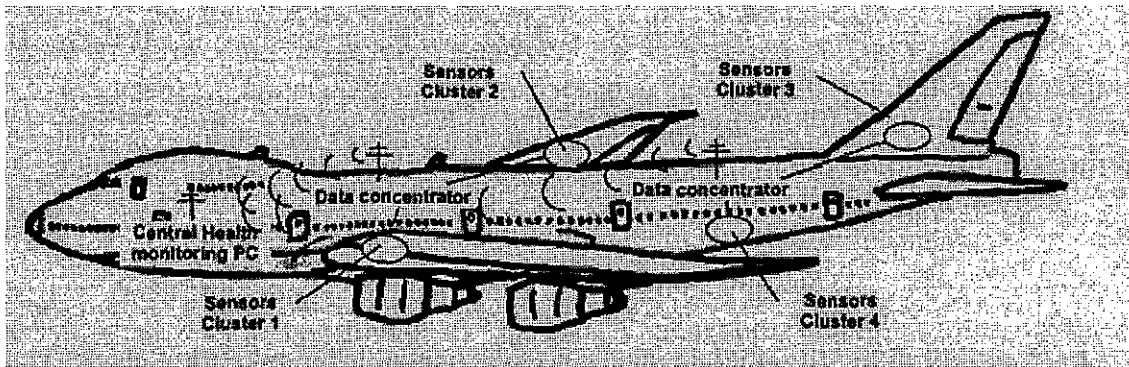


Figure 1: General concept for structural health monitoring of aircraft structures

Among several advanced candidate sensor technologies (e.g. piezoelectric ceramics and polymers, shape memory alloys, smart gels, MEMS, and NEMS) of significance to the development of SHMSs, optical fibre sensor technology is the most mature technology expected to see implementation in the near- to mid-term as part of aircraft structural health monitoring and prognostic management.

Optical fibre sensors have been developed to measure a variety of physical and chemical parameters including temperature, pressure, strain, load, position, thickness, humidity, pH, chemical reaction rates, and chemical concentration and characterization of species present in mixtures [2-12]. Variations of these parameters alter the optical and the geometric properties of the optical fibre influencing features (e.g. intensity, phase, or polarization) of light transmitted in

the fibre. Perturbations of the lightwave through the fibre can be interrogated using one of several techniques including scanning Fabry-Perot filters, spectrum analyzers, and interferometric techniques [13]. The selected technique depends on the transducer configuration. Among several configurations (e.g. extrinsic and intrinsic Fabry-Perot, long period grating, in-line fibre etalon), Bragg grating sensors are considered to be the most promising technology in the industry, particularly for civil and aerospace structures. These small size, EMI and RFI immune, lightweight, single-ended, quasi-distributed sensors exhibit high multiplexing capabilities (e.g. potentially hundreds to thousands of sensors on one optical fibre line) and multi-parameter sensing (e.g. strain, temperature, and pressure or humidity) [14-17]. These sensors are envisaged to be the nervous system of advanced aerospace structures and military platforms. Unlike their distributed-effect counter parts (e.g. Bernoulli, Mach-Zhender, Michelson) they possess high spatial resolution, placement flexibility, and temperature compensated strain mapping capability.

Regardless of the significant advances of fibre Bragg grating sensor technology for civil infrastructure applications such as bridges, buildings, dams, gas and oil pipelines and platforms, only modest progress toward the aerospace sector was made [18-21]. Complexity of electronics, moderate size of demodulation systems, the absence of reliable long-term and environmental data, and the lack of standards for implementation of sensing systems continue to be some of the major hurdles for implementation onto air platforms.

To further the understanding of technical and practical issues related to full implementation of fibre optic sensor technology onto aerospace and military platforms, and to ease some of the concerns presented by the aerospace community that include size, weight, power requirement, reliability, cost and performance, two experimental programs were initiated (1) evaluation of optical fibre sensors and (2) development of small size, low weight, highly multiplexed demodulation system [22]. Extensive overview of fibre Bragg grating technology and its applications can be found in the open literature including [13]. The work presented here, focuses on the experimental evaluation of fibre Bragg gratings for potential aerospace implementation. It uses a commercially available interrogation system (E-Teck 3100) with commercially fabricated gratings, the paper further documents findings on the use of a short-gauge in-fibre Bragg grating sensor for measurement of parameters relevant to aircraft structures and materials (e.g. pressure, temperature, strain, and curing rate). Details of experimental results can also be found in appropriate listed references. This paper further reflects lessons learned and addresses some remaining issues for successful implementation of SHMS's into air platforms and fibre optic smart structures.

2. PRINCIPLE OF FIBRE BRAGG GRATING

Optical Fibre Bragg Grating (FBG) technology credits its origin to the discovery of the photosensitivity in optical fibres by Hill *et al.* [23]. Fibre Bragg gratings are formed by generating a permanent periodic modulation in the fibre's core refractive index using various methods such as interferometry [24] or phase masks [25]. Metz *et al.* [24] demonstrated that a fine pitch grating could be impressed in a photosensitive germanium-doped optical fibre using a

high-intensity ultraviolet laser dual-beam interface, generally with a short wavelength (< 300 nm) of 248 nm, that spatially modulates the index of refraction of the fibre core. Adjusting the angle between the two coherent transverse illuminating beams that form the interference can control the pitch, Λ , of this grating. Once the incident light travels down the core of the Bragg grating fibre, the regions of changed refractive index reflect a narrow spectral band as illustrated in Figure 2. According to Bragg's law, the grating will only reflect a specific wavelength, Bragg wavelength (λ_B), which is given by

$$\lambda_B = 2n\Lambda \quad (1)$$

where n denotes the effective refractive index. The grating acts as a narrow band-stop optical filter. Any change in the refractive index or the grating pitch will result in a shift of the Bragg wavelength, as illustrated in Figure 3. Fibre Bragg grating response is determined by monitoring the variation in the grating's peak wavelength. This variation arises from a change in the pitch length of the grating, and/or a change in the effective refractive index, resulting from changes (e.g. local ambient temperature, load) applied to the fibre.

For surface mounted Bragg grating optical fibre sensors, the sensor response to axial loading depends on the variation of the Bragg wavelength, resulting from the photo-elastic and thermo-optic effect, respectively. The wavelength variation can be expressed as [26-27]

$$\Delta\lambda_B = \lambda_B \left\{ \left[1 - \left(\frac{n^2}{2} \right) [P_{12} - \nu(P_{11} + P_{12})] \right] \Delta\varepsilon + [\alpha + \xi] \Delta T \right\}; \quad \xi = \frac{\left(\frac{dn}{dT} \right)}{n} \quad (2)$$

where P_{ij} are Pockel's coefficients of the stress-optic tensor, ν is the fibre Poisson's ratio, α is the coefficient of thermal expansion, ξ is the thermo-optic coefficient, ΔT is the temperature variation and $\Delta\varepsilon$ is the strain variation. Assuming zero initial strain, the strain variation can be expressed as:

$$\varepsilon = \Delta\lambda_B / \lambda_B (1 - P_e) - (\alpha + \xi) \Delta T / (1 - P_e); \quad P_e = n^2 / 2 \{ P_{12} - \nu(P_{11} + P_{12}) \} \quad (3)$$

where P_e is the effective strain-optic coefficient, also known as the photo-elastic coefficient. For bulk values of $P_{11} = 0.126$, $P_{12} = 0.27$, $\nu = 0.17$, and $n = 1.46$ [28], the theoretical strain-optic coefficient and sensor gauge factor ($1 - P_e$) were determined to be 0.22 and 0.78, respectively. For fused silica at room temperature, α and ξ were determined to be $0.55 \times 10^{-6} / ^\circ\text{C}$ and $9.1 \times 10^{-6} / ^\circ\text{C}$ [29-30], respectively. Thus the sensitivity of the wavelength shift versus strain and temperature, for $\lambda_B = 1310$ nm, is approximately 1 pm/ $\mu\varepsilon$ and 13 pm/ $\mu\varepsilon$, respectively. These sensitivity values are confirmed experimentally as well.

To further the understanding of influencing parameters on Bragg grating optical fibre sensor response in the context of smart structures and SHM, several experimental evaluations were conducted employing commercially acquired Corning SMF-28 single in-fibre Bragg gratings

with FC/APC connector leads and Bragg wavelength of 1310 nm. A commercially acquired demodulation system (E-Tek 3100), that can interrogate three sensors independently, was employed for capturing, analyzing, and evaluating sensor response to variations in pressure, temperature, static, dynamic, and fatigue loading as well as Gr/Ep composite curing. Figure 4, shows the optical fibre sensor demodulation system with its three modules, including the connectors for the thermocouples used for external temperature monitoring.

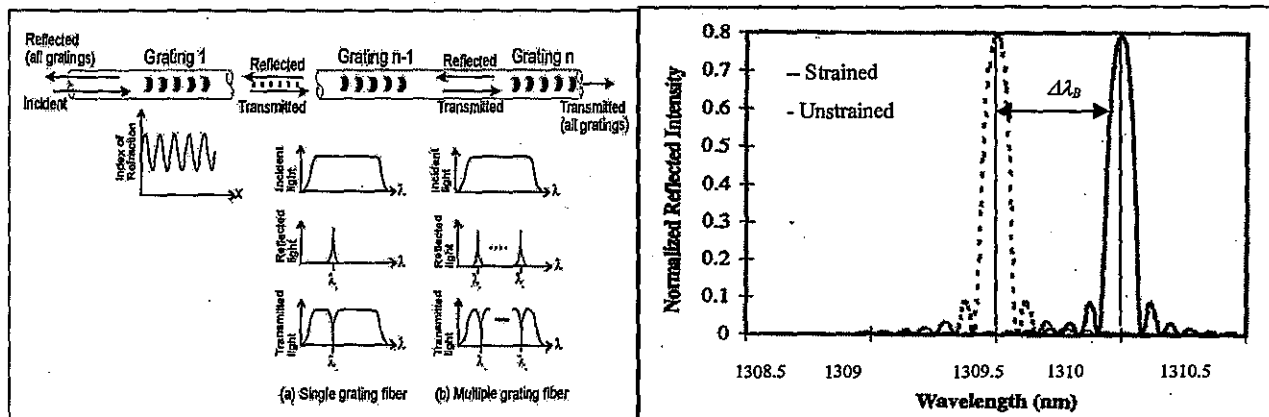


Figure 2: Bragg grating operating principle

Figure 3: Typical spectral response of FBG for $\lambda_B = 1310\text{nm}$

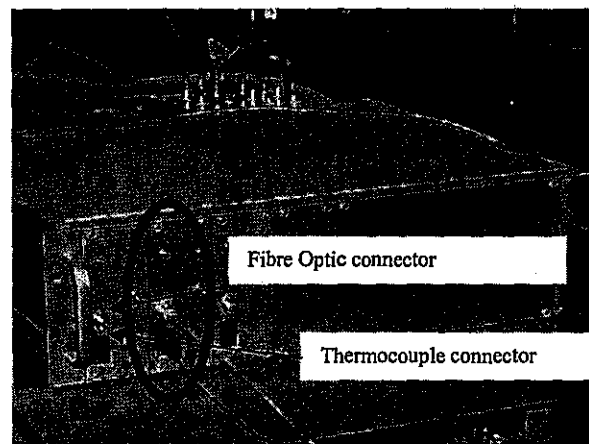


Figure 4: Fibre Bragg grating (FBG) demodulation and sensing system

3. FIBRE BRAGG GRATING (FBG) THERMAL RESPONSE

The thermal response of the FBG was evaluated under low (70°C) and high (300°C) temperature conditions. For low temperature experiments, the FBG sensor with a reference adjacent T-type thermocouple (TC) was placed in a Baxter DP-41 temperature-controlled vacuum oven (not shown). The FBG sensor was secured in the oven in a stress free environment. Both FBG and reference TC were heated from room temperature up to 70°C and subsequently cooled to 23°C at a rate of 1°C per minute. Data was acquired via the FBG

demodulation system and TC data-logging unit at five-second intervals during heating and sixty second intervals during cooling.

Table 1: Comparison of the Current (E-Tek 3100) FBG demodulation system and the one under development

Characteristic	Current system (E-Tek 3100)	Proposed system (current development)
Over all system size	320mm x 250mm x 165mm	50mm x 100mm x 120mm
Channel number	4	1 (stackable)
FBG on one Channel	1	>32
Weight	3kg	<500g
Cost	> CA\$29,000	< CA\$4,000
Resolution	1 pm	1 pm
Measurement Range	8500 $\mu\epsilon$	> 30 000 $\mu\epsilon$
Long term reliability	Not known	Proved in telecom industry
Scan frequency	1Hz	~250Hz
Power consumption	< 30W	<5W

For the high temperature experiment, the stress-free FBG sensor and the reference TC were secured to a plate placed in an autoclave (Figure 5). The mid-sized autoclave is a Baron-Blakeslee Inc. Model BAC-46 electrically heated, water-cooled pressure vessel capable of accurate automated control of typical cure cycles for composite parts processing. Its control variables include heating, cooling, applied pressure, vacuum ramps and stable set point holds. Instrumentation feed through ports and electrical connector panels were specially designed for accessing the vessel's interior to monitor sensors response and autoclave internal conditions. The autoclave was heated and cooled according to Hexcel AS4/3501-6 process cycle shown in Figure 6. Data was acquired at five seconds intervals during heating and cooling. Experiments were repeated 3 times for each temperature range.



Figure 5: Baron-Blakeslee Inc. Model BAC-46 autoclave set up for high temperature measurements

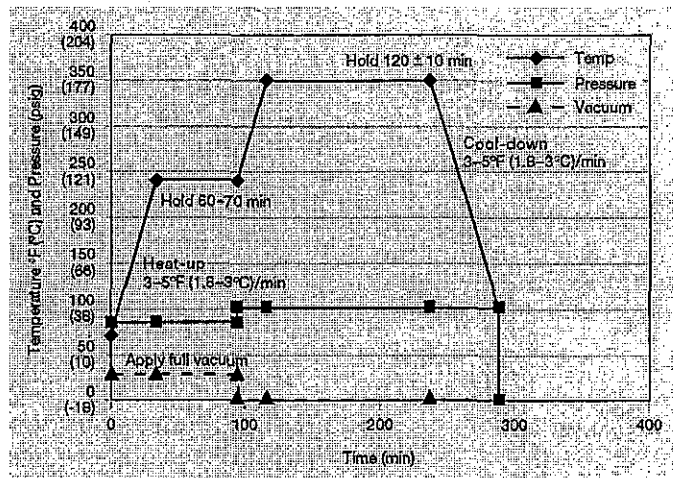


Figure 6: Hexcel AS4/3501-6 manufacturer process cycle

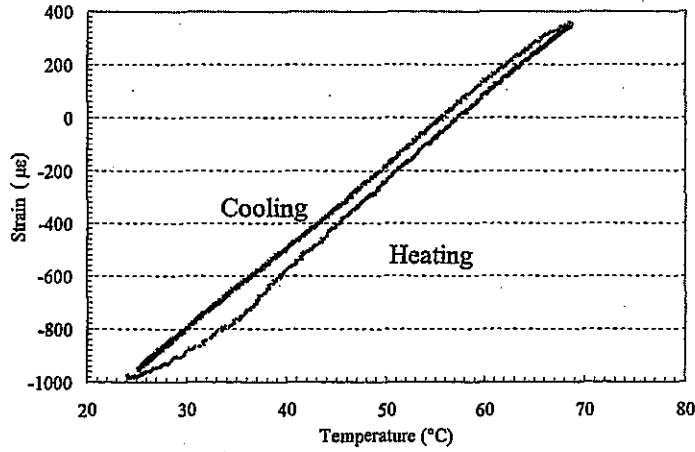


Figure 7.a: Bragg grating response to low temperature

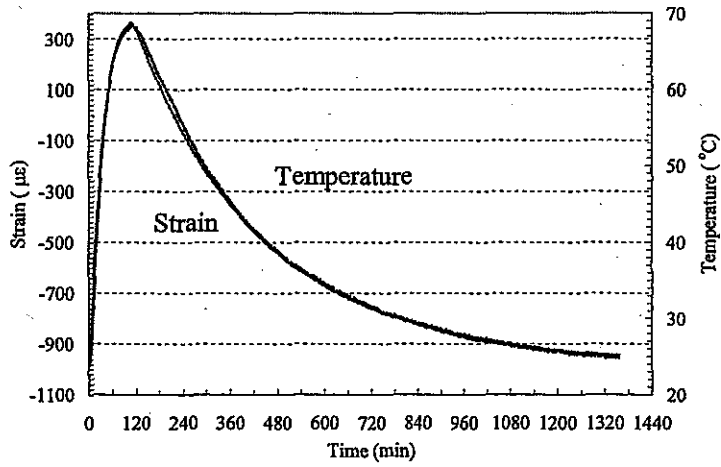


Figure 7.b: Bragg grating time response to low temperature

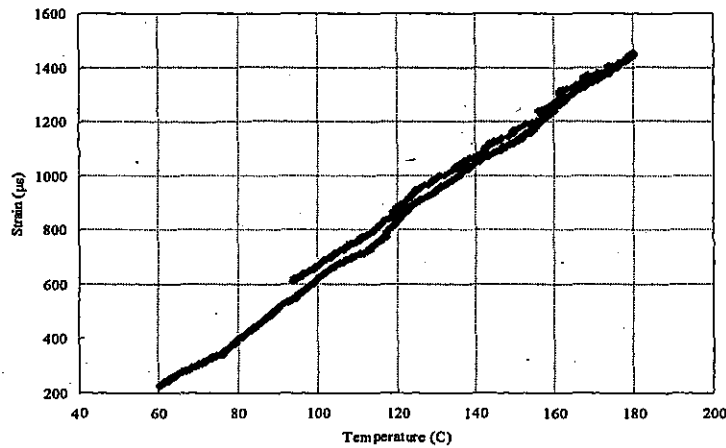


Figure 8: Bragg grating response to high temperature expose along the Hexcel AS4/3501-6 manufacturer process cycle of Figure 6

The thermal responses of the FBG sensor are shown in Figures 7 and 8, for low and high temperatures, respectively. Generally, FBG response correlates well with the TC response (Figure 7.b); however, nonlinearities were experienced during the heating phase. This is suspected to be due to the higher heating rate and the FBG low rate of heat absorption. Our current analysis (not shown) illustrated thermal dependence on fibre coatings and Bragg gratings center wavelength, particularly at low temperatures (-40°C).

4. FIBRE BRAGG GRATING (FBG) PRESSURE RESPONSE

To evaluate the FBG response and its sensitivity to pressure variation for potential composites process monitoring and control experiments were conducted for pressures up to 300 psi at constant room temperature. The Fibre Bragg grating was sealed in a pressure tube (filled with hydraulic fluid) shown in Figure 9 and subjected to pressure variation in steps of 10 psi taken at intervals of one second. The pressure was monitored using pressure transducer having sensitivity of 1v/1000psi. The temperature was also monitored using a T-type thermocouple. The sensor response shown in Figure 10 demonstrates the insensitivity of the Bragg gratings to pressure variation up to 300 psi. Any deviation from the nominal value of -32 $\mu\epsilon$ fell within the 3σ (3 $\mu\epsilon$) of the measured values and is a result of the resolution limitation of the data acquisition system and demodulation electronics. Temperature measurement was found to be constant at 23°C, thus not affecting the viscosity of the fluid in the pressure compartment and facilitating accurate pressure measurements. Similarly three experiments were conducted and illustrated the same outcome.

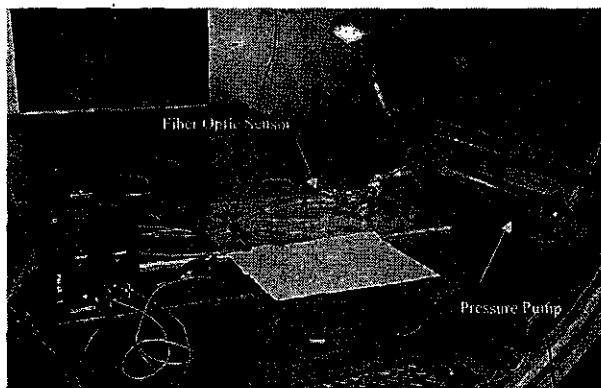


Figure 9: Pressure measurement set up

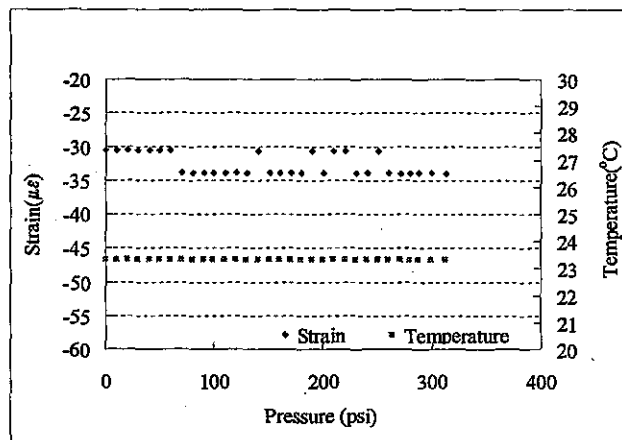


Figure 10: Bragg grating response to pressure variation up to 300 psi

5. FIBRE BRAGG GRATING (FBG) LOAD RESPONSE

In the development of fibre optic sensing technology, strain measurement continues to be the leading parameter of interest, particularly for smart structures and structural health monitoring. The FBG response to applied static, dynamic, and fatigue loadings is experimentally evaluated.

5.1. Static Fibre Bragg Grating Response

An aluminum 7075-T6 tensile specimen was instrumented with bondable FBG and two 350 Ω resistive foil strain gauges (RSG), placed on the front (RSG4) and back (RSG3) of the panel. The instrumented panel with dimensions 19x2x¼ in³ was placed in an MTS 880 load frame shown in Figure 11 and loaded in tension and compression at loads ranging from -4000 lbs to 10000 lbs. RSG4 was employed to validate the FBG sensor measurements and RSG3 was employed to detect any misalignment or bending in the specimen. During experiments, the temperature was maintained constant at room temperature. Strain and temperature measurements were recorded for 19 seconds at load intervals of 500 lbs. Theoretical and experimental sensor responses along with FBG demodulation system calibration curves are shown in Figure 12.

Results show that both front strain gauge and FBG sensor correlate well with theoretical strain data (e.g. deviation of 1.5% for the RSG4 and 2.1% for FBG) during tensile loading. During compression loading the deviation of 2.3% for the FBG response remained consistent with tension, while the foil strain gauge deviations increased to 5.1% and 5.7%, respectively for RSG4 and RSG3, respectively. Generally, the deviation is within experimental expectation and the output falls within the 3 σ ($\pm 3 \mu\epsilon$) variation, such deviation can be attributed to specimen buckling. Tests were also repeated three times to validate the confirmed process and reproducibility of the results.

5.2. Dynamic Fibre Bragg Grating Response

Employing the same experimental setup of Figure 11 and disengaging the load frame upper grip (cantilevered beam configuration), free vibration of the instrumented panel was initiated by applying small transverse displacement. The response of the FBG sensor and the foil strain gauge (RSG4) are shown in Figure 13. Dynamic response of the FBG was determined to fall within 10% of theoretical value for the first vibration mode and within 13% for the second mode, which both are within the expected level of experimental variation [31].

5.3. Fatigue Fibre Bragg Grating Response

Employing the same experimental setup of Figure 11 with a modified test article, the response of FBG to crack growth is investigated. A 0.04 in wire Electrical Discharge Machined (EDM) notch was initiated on both side of a 0.125 in whole centered in a 0.05x4x12 in³ instrumented Al. 7075-T6 specimen to simulate a crack initiation. A FBG sensor, a resistive strain gauge (RSG) and a crack growth gauge were instrumented on the article as shown in Figure 14. Sensors were placed symmetrically in constant strain regions to allow for accurate comparison of sensor performance. An ANSYS finite element analysis was performed to determine these constant strain regions. Figure 15, represents both RSG and FBG responses to crack growth. The crack size is determined by using the crack growth gauge with strand spacing

of 1 mm. Results illustrate the capability of the FBG to track the crack as it grows (Figure 15 represents raw data not intended for direct comparison.)

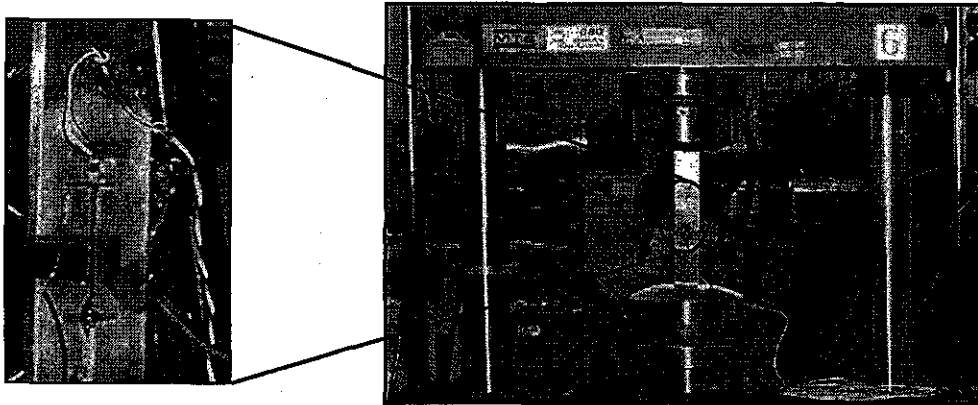


Figure 11: Experimental set up for fibre Bragg grating load monitoring

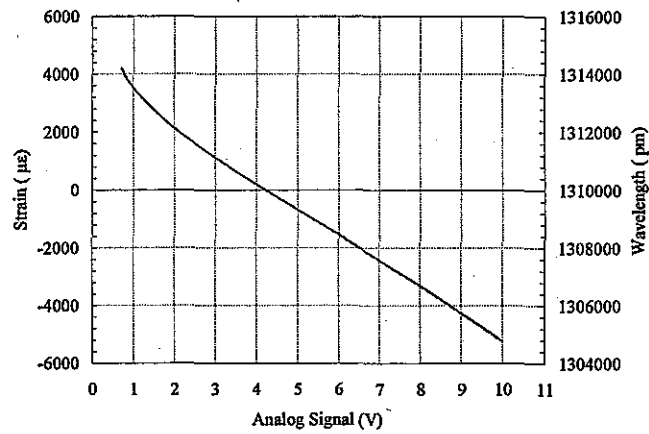


Figure 12.a: Bragg grating calibration curve for static load

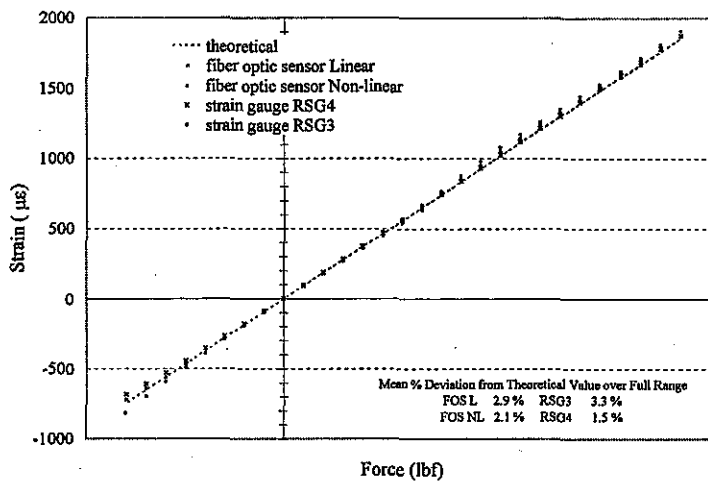


Figure 12.b: Bragg grating response to static load

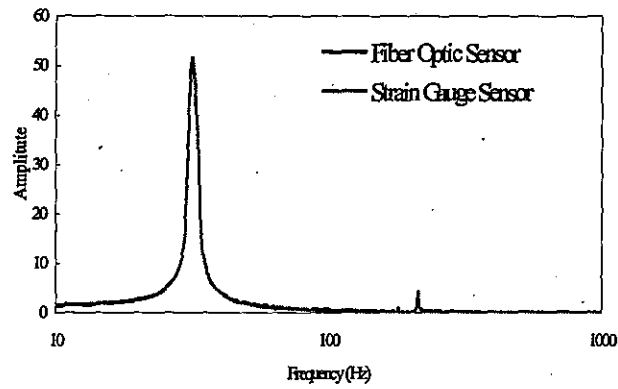


Figure 13. Free vibration frequency response of FBG sensor

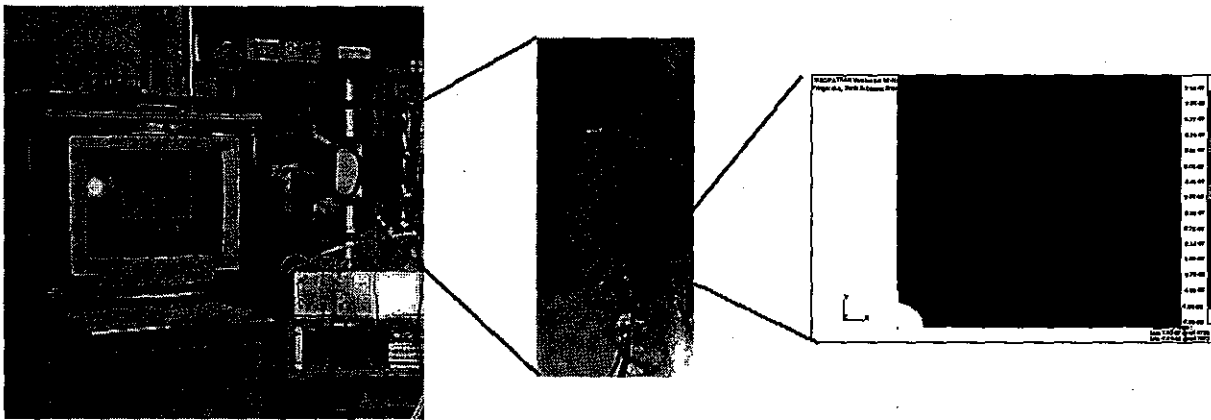


Figure 14: Experimental set up for crack growth monitoring using fibre Bragg grating sensor.

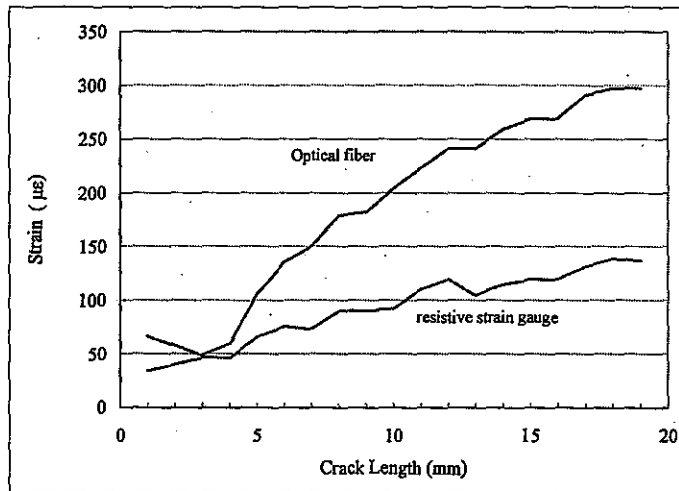


Figure 15: Fibre Bragg grating response to crack growth

Mrad *et al.* [31] evaluated the reliability, durability and fatigue-life performance of FBG under cyclic loading at frequency of 20 Hz and peak-to-peak amplitudes from 500 lbs to 5000 lbs. They observed that over two million cycles, little to no degradation in the sensor output was observed. They reported less than 1% change of the strain over load after the two million cycles. They also recommended conducting such evaluation under more realistic condition, representative of the operational environment of the aircraft (e.g. grating response under hygrothermal variations.)

6. FIBRE BRAGG GRATING (FBG) COMPOSITE PROCESSING RESPONSE

A 20-ply unidirectional Hexcel AS4/3501-6 pre-preg carbon fibre/epoxy (Gr/Ep) lay-up with nominal overall panel dimensions of 4x12 in² was cured in an autoclave environment (Figure 5) following the manufacturer process cycle shown in Figure 6. A FBG, a resistive strain gauge, and a T-type thermocouple were embedded into the composite panel along the direction of the carbon fibres, 2-plyes away from the outer surface. Standard manufacturing procedures were conducted in the preparation of pre-preg carbon fibre lay-up and vacuum bagging. Slight modification was required to accommodate embedded sensor instrumentation wiring and cabling. Special attention was given to vacuum debulking which was conducted after every 4 plies of lay-up. This procedure is implemented to eliminate potential entrapment of air and minimize final part voiding and subsequent porosities.

Figure 16 shows the manufactured final composite part with embedded FBG, RSG, and TC sensors. This figure also shows an embedded piezoelectric actuator, with lead wires, used for work on active vibration of smart structures. It illustrates the effect of embedding sensors and actuators into composite materials on the final part quality. Figure 16 further illustrates the temperature, resistive and fibre optic strain gauges response during composite part curing. Assessment of these results demonstrates that some level of mechanical strain is detected between 2000 and 14000 seconds indicating that the curing process is taking place. Particular interest is the observed strain overshoot (899 $\mu\epsilon$) at 2.07 hrs and the strain reduction (839 $\mu\epsilon$) at 3.3 hrs. At this level the strain becomes constant indicating the end of cure. Such technique can provide optimal cure cycle and potentially reduce process time and part rejection and cost. One of the experienced limitation of the FBG is that the sensors, prior to embedment, undergone a preconditioning stage. That is, the sensor was subjected to a temperature cycle identical to that used for the AS4/3501-6 pre-preg carbon fibre/epoxy prior to its embedment into the part to be monitored. This limitation can be addressed at the manufacturing stage of the FBG and the use of temperature-compensated dual gratings as proposed by several researchers [32-35].

A qualitative analysis of fibre Bragg grating embedment into 10 plies unidirectional Graphite/Epoxy (AS4/3501-6) demonstrated that optical fibres should be embedded parallel to graphite fibers for reduced intrusiveness (Figure 17). If optical fibres are placed perpendicular to the graphite fibres, discontinuities are introduced and a reduction of strength is expected. Research [36] conducted on studying the adverse effects of embedded optical fibres on the strength of composite materials, showed that, for fibre embedded along the direction of graphite fibre, negligible reduction in tensile stiffness and static strength was observed. However, a 10%

reduction of compressive strength was observed when optical fibres are embedded into composite laminates.

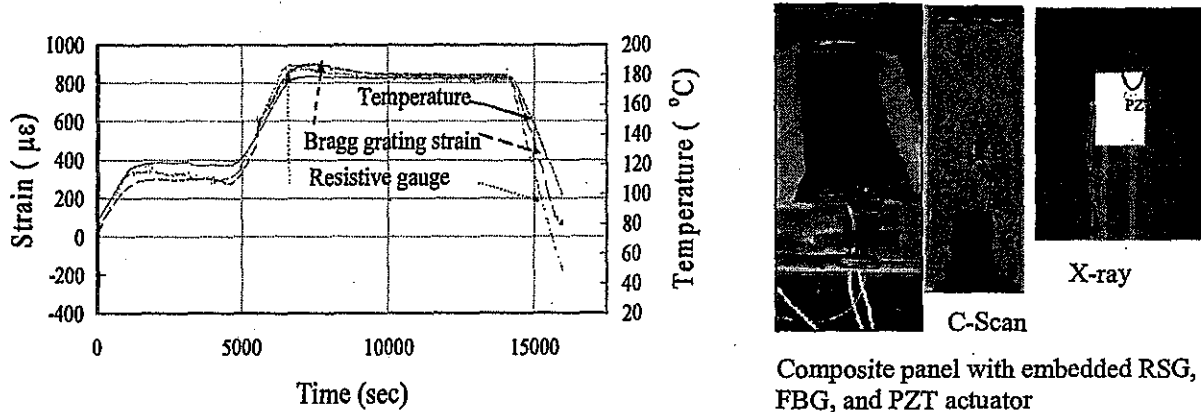


Figure 16: Bragg grating fibre optic composite cure monitoring

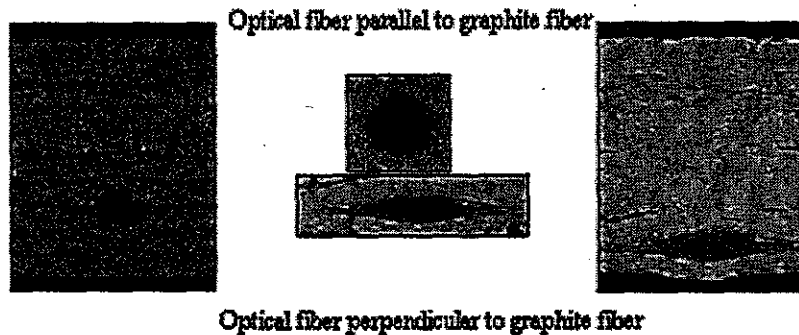


Figure 17: Embedded optical fibre into 10 plies unidirectional Gr/Ep AS4/3501-6

7. SMART STRUCTURES AND STRUCTURAL HEALTH MONITORING SYSTEM (SHMS) IMPLEMENTATION

Results presented above, emphasized the performance and response evaluation of in-fibre single Bragg grating sensors for potential integration into a multi-functional sensory system as part of an aircraft SHMS. Significant research exist addressing FBG multiplexing, temperature compensation and thermal dependence, bonding and embedding, egress and ingress, etc. The proposed SHMS architecture is to employ an on-board computer system that detects, monitors and assesses the structural health of the aircraft continuously or as required and make information available to the crew, command and control, logistics and maintenance support, and/or direct support. Localized health of the aircraft is assessed through diagnostics and onboard sensors (S_i). Overall health condition is assessed through diagnostics and prognostics of the cluster sensors (C_i) and local wireless networks. The aircraft health status is periodically transmitted through telemetry, from the central processor (C) to command and control system to

enable battle readiness assessment and to the maintenance support to prepare for maintenance; if anomalies are reported. Figure 18, represents a SHMS architecture.

Due to the high multiplexing capability, the potential for wider surface coverage and integration into structural components in the early stages of design and development, optical fibre Bragg grating sensors provide a potentially cost effective approach to aircraft structural health monitoring and prognostics management. The feasibility of using this technology for the measurement of several parameters has also been demonstrated in this document for single gratings. However, our current investigation focuses on the development of miniaturized demodulation system for highly multiplexed Bragg grating wireless sensor networks. As we continue to develop both sensors and demodulation technology, some significant practical implementation issues impacting the integration of this technology into aerospace platforms are identified.

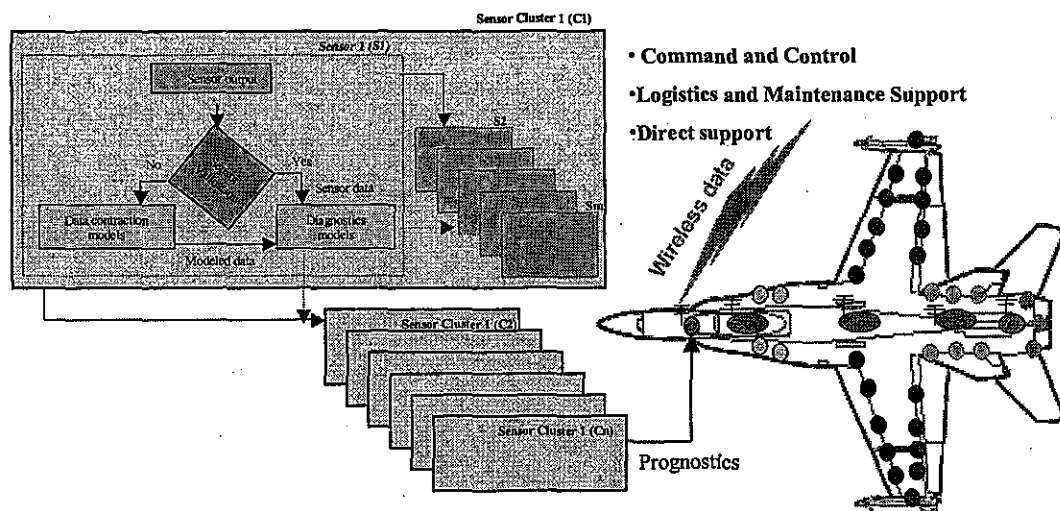


Figure 18: A schematic of an aircraft SHMS architecture

7.1. Bragg Grating Sensor Performance and Integration

- a. Establish long-term performance, functional reliability and affordability of sensor systems over operational life of aircraft (> 30 years) and under operational conditions (e.g. temperatures between -65°C and 65°C).
- b. Develop a universal reduced size reliable, robust, affordable, lightweight demodulation system for interrogating EFPI, FBG, and LPG sensors. The system should be flexible for quasi-distributed multi-parameters sensing with desired spatial distribution (e.g. thousands of sensors with few millimeters to centimeters separation between transducer elements).
- c. Develop innovative methodologies and standards for sensor protection at the ingress/egress points without adding complexity in part manufacturing and assembly and without altering airworthiness standards and certification requirements.

- d. Develop modelling and simulation tools for multiplexed sensor networks performance evaluation and self-diagnostics and sensors output evaluation and interpretation in embedded configurations.
- e. Establish and develop advanced signal processing tools based on artificial neural networks and artificial intelligence for reduced sensor network and enhanced system reliability and efficiency.

7.2. Implementation Of Structural Health Monitoring System (SHMS)

- a. Develop an understanding of fault progression processes for critical failure modes for high value components suitable for prognostics.
- b. Develop a distributed architecture SHMS as opposed to centralized decision system. This offers the desired reliability, robustness and scalability and may introduce new bottlenecks such as the network bandwidth and synchronization requirements.
- c. Properly establish and develop characteristics of the SHMS architecture including scalability, legacy systems, openness, flexibility, robustness, extendibility and intelligent monitoring.
- d. Develop metrics for the SHMS architectural evaluation assuming it contains sensors, processors, communication links (and networks), software, processes and storage or I/O units.
- e. Develop modelling and analysis tools requiring optimal communications between local sensors and global sensor clusters to reduce power consumption and communication overheads.
- f. Develop information fusion and reasoner models for information management and communication.
- g. Develop secure and reliable wireless on-board and off-board communication that does not interfere with other aircraft electronics.
- h. Ensure that wireless data transfer is done securely and not subjected to interruption in the presence of disturbances (e.g. EMI) including aircraft structural components and systems (i.e. communication should be unaffected within the aircraft.)
- i. Identify and implement user friendly, cost effective, reliable, signal interpretation and analysis tools.
- j. Ensure that the SHMS relates accurate decisions having no adverse impact on planned missions or operational requirements.

8. CONCLUSIONS

An experimental evaluation on the use of short-gauge in-fibre Bragg grating sensors for potential integration in smart structures and advanced structural health monitoring systems has been conducted. These fibre Bragg grating sensors were found to correlate well with conventional sensor technology for temperature, static, dynamic, crack growth and cure monitoring. They were found to be insensitive to pressure up to 300 psi and had a minimum impact on the structural integrity when embedded parallel to the host fibres into composite laminates. The paper further identified some of the critical key steps requiring further consideration for successful development and implementation of a SHMS for aerospace

structures and air platforms. In doing so, this experimental evaluation has furthered the understanding of the technical and practical issues, and identified the merit of the technology for aircraft and military platforms. As a result of the developed understanding, current efforts are under way to develop multi-parameters SHMS based on highly multiplexed fibre Bragg gratings and miniaturized interrogation wireless units.

9. ACKNOWLEDGEMENTS

This work was conducted under collaborative agreement between Defence R&D Canada (DRDC) of the Department of National Defence (DND) and the Institute for Aerospace Research (IAR) of the National Research Council Canada (NRC). The technical support of Mr. Ron Gould, Mr. Brian Moyes, Mr. Tony Marincak, Mr. Thomas Benak, and Dr. Guoqin Shi of IAR is acknowledged and very much appreciated.

10. REFERENCES

1. V. Giurgiutiu, A. Zagrai, and J.J. Bao, Piezoelectric Wafer Embedded Active Sensors for Aging Aircraft Structural Health Monitoring, *Structural Health Monitoring*, 1 (1) (2002) 41-61.
2. D.A. Krohn, *Fibre Optic Sensors: Fundamentals and Applications*, 3rd edition, Instrument Society of America, North Carolina, 2000.
3. C.D. Butter and G.B. Hocker, Fibre Optics Strain Gauge, *Appl. Opt.*, 17 (18) (1978) 2867-2869.
4. Z. Zhou and M.A. Arnold, Response Characteristics and Mathematical Modelling for a Nitric Oxide Fibre-Optic Chemical Sensor, *Analytical Chemistry*, 68 (1996) 1748-1754.
5. D. Stadnik and A. Dybko, An Intrinsic Fibre Optic Chemical Sensor Based on Light Coupling Phenomenon, *Sensors and Actuators B: Chemical*, 107 (1) 2005 184-187.
6. G.F. Fernando, Fibre Optic Sensor Systems for Monitoring Composite Structures, *Reinforced Plastics*, 49 (11) 2005 41-49.
7. H-K. Kang, H.-J. Bang, C.-S. Hong and C.-G. Kim, Simultaneous Measurement of Strain, Temperature and Vibration Frequency Using a Fibre Optic Sensor, *Meas. Sci. Technol.* 13 (2002) 1191-1196.
8. C.C. Shing, An investigation of chirped fibre Bragg gratings Fabry-Perot interferometer for sensing applications, Cranfield University, Centre for Photonics and Optical Engineering, Optical Sensors Group, PhD Thesis, 2005.
9. B. Zhang, D. Wang, S. Du and Y. Song, An Investigation of a Fibre Optic Sensor In The Composite Cure Process, *Smart Materials and Structures*, 8 (1999) 515-518.
10. A.J. Rogers, Distributed Optical-Fibre Sensors for the Measurement of Pressure, Strain and Temperature, *Journal of the Institution of Electronic and Radio Engineers*, 58 (5-Supplement) (1988) S113-S122.
11. W.N. MacPhersona, M.J. Gander, R. McBridea, J.D.C. Jonesa, P.M. Blanchardb, J.G. Burnettb, A.H. Greenawayb, B. Manganc, T.A. Birksc, J.C. Knightc and P.St.J. Russelld, Remotely Addressed Optical Fibre Curvature Sensor Using Multicore Photonic Crystal Fibre, *Optics Communications*, 193 (1-6) 2001 97-104.
12. W.J. Bock and W. Urbanczyk, Multiplexing of White-Light Interferometric Fibre-Optic Sensors For Hydrostatic Pressure and Temperature Measurements, *Optical Society of America*, 12th International Conference on Optical Fibre Sensors, Williamsburg, Virginia, Technical Digest, (1997) October 28-31.
13. N. Mrad, Optical Fibre Sensor technology: Introduction and Evaluation and Application, *the Encyclopedia of Smart Materials*, John Wiley and Sons, Inc., 2 (2002) 715-737.
14. S.E. Kanellopoulos, V.A. Handerek and A.J. Rogers, Simultaneous Strain and Temperature Sensing with Photo Generated in-Fibre Gratings, *Optics Letters*, 20 (3) (1995) 333-335.
15. T. Liu, G.F. Fernando, L. Zhang, I. Bennion, Y. Rao and D.A. Jackson, Simultaneous Strain and Temperature Measurement Using an Integrated Fibre Bragg Grating/Extrinsic Fabry-Perot Sensor, *Proceedings of SPIE Conference on Sensory Phenomena and Measurement Instrumentation for Smart Structure and Materials*, San Diego, California, 3330 (1998) 324-331.

16. K.M. Tana, C.M. Taya, S.C. Tjina, C.C. Chana and H. Rahardjoa, High Relative Humidity Measurements Using Gelatin Coated Long-Period Grating Sensors, *Sensors and Actuators B: Chemical*, 110 (2) 2005 335-341.
17. K. Totsu1, Y. Haga and M. Esashi, Ultra-miniature Fiber-optic Pressure Sensor Using White Light Interferometry, *J. Micromech. Microeng.* 15 (2005) 71-75.
18. M. Trutzel, K. Wauer, D. Betz, L. Staudigel, O. Krumpolz, H.C. Mühlmann, T. Müllert and W. Gleine, Smart sensing of aviation structures with fiber-optic Bragg grating sensors, *Proc. SPIE*, Newport Beach, CA, 3986 (2000) 134-143.
19. D.C. Betz, L. Staudigel, M. Trutzel, M. Schmuecker, E. Huelsmann and U. Czernay, Test of a fiber Bragg grating sensor network for commercial aircraft structures, *Proc. 15th Int. Conf. Optical Fiber Sensors*, Portland, OR, (2002) 55-58.
20. P. Foote and I. Read, Applications of optical fibre sensors in aerospace: The achievements and challenges, *Proc. SPIE-Int. Soc. Opt. Eng.*, Glasgow, U.K., 4074 (2000) 246-261.
21. K. Wood, T. Brown, R. Rogowski and B. Jensen, Fiber optic sensors for health monitoring of morphing airframes: I. Bragg grating strain and temperature sensor, *2000 smart mater. struct.* (9), (2000) 163-169.
22. N. Mrad and G. Z. Xiao, Multiplexed fibre Bragg gratings for potential aerospace applications, *Proceedings of the 2005 international conference on mems, nano, and smart systems (icmens 2005)*, banff, alberta, canada, july 24 - 27, (2005) 359-363.
23. K.O. Hill, Y. Fujii, D.C. Johnson and B.S. Kawasaki, Photosensitivity in Optical Fibre Waveguides: Application to Reflection Filter Fabrication, *Applied Physics Letters*, 32 (10) (1978) 647-649.
24. G.R. Meltz, W.W. Morey and W.H. Glenn, Formation of Bragg Gratings in Optical Fibres by a Transverse Holographic Method, *Optic letters*, 14 (15) (1989) 823-825.
25. K.O. Hill, B. Malo, F. Bilodeau, D.C. Johnson and J. Albert, Bragg gratings fabricated in mono-mode photosensitive optical fibre by UV exposure through a phase mask, *Appl. Phys. Lett.* 62 (1993) 1035-1037.
26. A.D. Kersey, M.A. Davis, H.J. Patrick, M. LeBlanc, K.P. Koo, C.G. Askins, M.A. Putnam and E.J. Friebele, Fibre grating sensors, *J. Lightwave Tech.* 15 (1997) 1442-1462.
27. N. Mrad, R.G. Melton and B.T. Kulakowski, Performance of Optical Sensors in the Control of Flexible Structures, *Journal of Intelligent Material Systems and Structures*, 8 (11) (1997) 920-928.
28. C.E. Lee, H.F. Taylor, A.M. Markus and E. Udd, Optical-fibre Fabry-Perot Embedded Sensor, *Optics Letters*, 14 (21) (1989) 1225-1227.
29. M.B. Reid and M. Ozcan, Temperature Dependence of Fibre Optic Bragg Gratings at Low Temperatures, *Opt. Eng.* 37 (1) (1998) 237-240.
30. X.C. Li, F. Prinz and J. Seim, Thermal behavior of a Metal Embedded Fibre Bragg Grating Sensor, *Smart Mater. Struct.* 10 (2001) 575-579.
31. N. Mrad, S. Sparling and J. Laliberté, Strain Monitoring and Fatigue Life of Bragg Grating Fibre Optic Sensors, *Proceedings of the International Society for Optical Engineering - SPIE 6th Annual International Symposium on Smart Structure and Materials, Sensory Phenomena and Measurement Instrumentation for Smart Structures and Materials*, Newport Beach, California, USA, 3670 (1999) 82-91.
32. M. Giordano, A. Laudati, J. Nasser, L. Nicolais, A. Cusano and A. Cutolo, Monitoring by a single fiber Bragg grating of the process induced chemo-physical transformations of a model thermoset, *Sensors Actuators A*, 113 (2004) 166-73.
33. E. Chehura, M. Kazilas, S. W. James, I.K. Partridge and R. P. Tatam Strain, Development in Curing Epoxy Resin and Glass Fiber/Epoxy Composites Monitored by Fibre Bragg Grating Sensors in Birefringent Optical Fibre, *Smart Materials and Structures*, 14 (2005) 354-362.
34. W. Jin, W.C. Michie, G. Thursby, M. Konstantaki and B. Culshaw, Simultaneous measurement of strain and temperature: error analysis, *Opt. Eng.* 36 (1997) 98-109.
35. B.A. Childers, M.E. Froggatt, S.G. Allison, T.C. Moore, D.A. Hare, C.F. Batten and D.C. Jegley, Use of 3000 Bragg grating strain sensors distributed on four eight-meter optical fibers during static load tests of a composite structure, *Proc. SPIE-Int. Soc. Opt. Eng.*, Newport Beach, CA, 4332 (2001) 133-142.
36. NAL Research Highlight, <http://www.nal.go.jp/struct/eng/kakushin/E-research.html>, (1997).